



An evaluation of the general composition and critical raw material content of bauxite residue in a storage area over a twelve-year period

Patricia B. Cusack^{a, b}, Ronan Courtney^{a, b}, Mark G. Healy^c, Lisa M.T. O' Donoghue^d, Éva Ujaczki^{b, d, e, *}

^a Department of Biological Sciences, University of Limerick, Castletroy, Co. Limerick, Ireland

^b The Bernal Institute, University of Limerick, Castletroy, Co. Limerick, Ireland

^c Civil Engineering, National University of Ireland, Galway, Ireland

^d School of Engineering, University of Limerick, Castletroy, Co. Limerick, Ireland

^e Department of Applied Biotechnology and Food Science, Faculty of Chemical Technology and Biotechnology, Budapest University of Technology and Economics, Műegyetem rkp. 3, 1111 Budapest, Hungary

ARTICLE INFO

Article history:

Received 7 June 2018

Received in revised form

28 September 2018

Accepted 9 October 2018

Available online 9 October 2018

Keywords:

Bauxite residue

Bauxite residue disposal area

Reuse value

Critical raw materials

ABSTRACT

Bauxite residue, the by-product produced in the alumina industry, is being produced at an estimated global rate of approximately 150 million tonnes per annum. Currently, the reuse of bauxite residue is low (~2%), due to limitations associated with its alkalinity, salinity, low solid content, fine particle size and potential leaching of metal(loid)s. It has been identified as a potential secondary source for critical raw materials such as vanadium, gallium and scandium, which currently have an associated supply risk and high economic cost within Europe. However, there is an uncertainty regarding the possible variation in these and other physico-chemical, elemental and mineralogical parameters within bauxite residue disposal areas. This paper aimed to address this knowledge gap by examining the variation of these parameters in a bauxite residue disposal area (BRDA) over a twelve-year period. The general composition did not vary greatly within the bauxite residue examined, with the exception of pH and electrical conductivity, which ranged from 10 ± 0.1 to 12.0 ± 0.02 and from 0.4 ± 0.01 to $3.3 \pm 0.2 \text{ mS cm}^{-1}$, respectively. The bauxite residue contained critical raw materials, of which the amount of vanadium, gallium and scandium did not vary significantly over time. The vanadium and gallium were present in larger amounts compared to other European bauxite residues. On average the vanadium, gallium and scandium content measured in the bauxite residue samples were 510 ± 77.8 , 107 ± 7.3 and $51.4 \pm 5.4 \text{ mg kg}^{-1}$, respectively. This shows promise for the potential reuse of bauxite residue as a secondary source for critical raw materials and also indicates that BRDAs may be potential mines for critical raw material extraction.

© 2018 Elsevier Ltd. All rights reserved.

1. Introduction

Bauxite residue (red mud) is the by-product generated during the extraction of alumina from bauxite ore using the Bayer Process (Kirwan et al. 2013), and is currently being produced at a global rate of 150 Mt per annum, adding to the 3 Bt already in storage worldwide (Evans, 2016). Currently, less than 2% of the bauxite residue generated annually is being reused (Ujaczki et al. 2018), with the remaining ~98% going into bauxite residue disposal areas (BRDAs) (Burke et al. 2013). The average cost of disposing and managing of bauxite residue in storage is 1–2% of the alumina price for the

alumina refinery (Tsakiridis et al. 2004).

Current best practice guidelines for the storage of bauxite residue is to use dry-stacking, a method which involves the thickening of the bauxite residue slurry from the Bayer process, using a filter press or vacuum filtration (depending on the refinery), before being spread in layers in the BRDA (Power et al. 2011; Evans, 2016). Depending on the nature of the bauxite ore used, some refineries operate a separation technique (Evans, 2016), which allows the bauxite residue to be separated into two main size fractions: a fine fraction (particle size $<100 \mu\text{m}$) and a coarse fraction (particle size $>150 \mu\text{m}$) (IAI, 2015; Jones et al. 2012). Bauxite residue is typically characterised as being highly alkaline, saline and composed of mainly fine particles comprised of a wide range of metal(loid)s and minerals (Gräfe et al. 2011). This poses challenges in the long-term management of BRDAs in terms of protecting the

* Corresponding author. The Bernal Institute, University of Limerick, Castletroy, Co. Limerick, Ireland.

E-mail address: eva.ujaczki@ul.ie (É. Ujaczki).

Nomenclature			
Al	aluminium	kV	kilovolt
AlO(OH)	boehmite	La	lanthanum
Al(OH) ₃	aluminium hydroxide hydrate	Lu	lutetium
Al ₂ O ₃	aluminium oxide	1M	1 M
As	arsenic	mA	milliamp
BRDA(s)	bauxite residue disposal area(s)	Mo	molybdenum
Bt	billion tonnes	MPa	megapascal
CaO	calcium oxide	Mt	million tonnes
Ca(OH) ₂	slaked lime	N	nitrogen
CaTiO ₃	perovskite	NaOH	sodium hydroxide
Cd	cadmium	Nd	neodymium
Ce	cerium	Ni	nickel
Co	cobalt	P	phosphorus
CO ₂	carbon dioxide	ρ _b	bulk density (g cm ⁻³)
CRM(s)	critical raw material(s) (mg kg ⁻¹)	PGM	platinum group metals
Cr	chromium	PVDF	polyvinylidene difluoride
Cu	copper	pH	pH(pH unit)
DSC	differential scanning calorimetry (mW)	Pr	praseodymium
Dy	dysprodim	PSA	particle size analysis (µm and in % of the total particle distribution)
EC	electrical conductivity (mS cm ⁻¹)	REE(s)	rare earth element(s) (mg kg ⁻¹)
EDS	energy-dispersive x-ray spectroscopy (weight %)	REO(s)	rare earth oxide(s)
Er	erbium	Sc	scandium
Eu	europium	SEM	scanning electron microscope (µm)
EU	European Union	SiO ₂	silicon oxide
Fe	iron	Sm	samarium
FeO(OH)	goethite	Tb	terbium
Fe ₂ O ₃	iron oxide	TGA	thermogravimetric analysis (mg)
Ga	gallium	Ti	titanium
Gd	gadolinium	TiO ₂	titanium oxide
HCl	hydrochloric acid	Tm	thulium
HNO ₃	nitric acid	Tn	terbium
Ho	holmium	V	vanadium
ICP-OES	inductively coupled plasma optical emission spectrometer	XRD	x-ray diffraction (°2θ)
In	indium	XRF	x-ray fluorescence (%)
Kα	k alpha	Y	yttrium
		Yb	ytterbium

surrounding environment (Higgins et al. 2017; Kong et al. 2017a; b), due to the high alkalinity, increased risk of dust pollution (due to the fine particles), and leaching of trace elements (Wang et al. 2015; Kong et al. 2017a,b). The disposal conditions and management of residue in a BRDA is dependent on many factors such as location, climate, engagement with local communities and stakeholders (IAI, 2015) and involves licencing permits from regulatory authorities (such as the Environmental Protection Agency). For example, European operators must meet the requirements according to the European List of Waste and Directive (EU Communities, 1999,2000). As a result of this, some refineries implement neutralisation techniques prior to disposal, such as carbon dioxide (CO₂) sparging of residues (Cooling, 2007) or post disposal through the use of atmospheric carbonation (mud farming) with amphirolling (Evans, 2016) in the BRDA, which helps in the neutralisation, dewatering and compaction of the bauxite residue (Evans, 2016; Gomes et al. 2016; Higgins et al. 2016; Zhu et al. 2016a; b), reducing both alkalinity and moisture content, which are two limitations to the re-use of bauxite (Evans, 2016).

Traditionally, the reuse of bauxite residue has focussed on construction applications such as cementitious application (Pontikes and Angelopoulos, 2013; Nikbin et al. 2018). Some other reuse options for bauxite residue have included polymers (Hertel

et al. 2016), ceramics (Pontikes et al. 2009) and catalysts (Wang et al. 2008); adsorbents for wastewater treatment (Bhatnagar et al. 2011), particularly for the removal of arsenic (As) (Arco-Lázaro et al. 2018), chromium (Cr) (Dursun et al. 2008), nickel (Ni) (Hannachi et al. 2010), copper (Cu) (Atasoy and Bilgic, 2018), cadmium (Cd) (Ha et al. 2017) and phosphorus (P) (Cusack et al. 2018), as well as applications as potential soil ameliorants (Ujaczki et al. 2015). More recently and due to the demand of critical raw materials (CRMs), particularly the rare earth elements (REEs), studies have examined the potential of bauxite residue as a secondary source of these materials and their potential economic value (Gomes et al. 2016; Xue et al. 2016; Ujaczki et al. 2017).

Within the European Union (EU), the 'Raw Materials Initiative' ensures that Europe secures and sustains an affordable supply of CRMs which are identified as being of high economic importance and having a risk to their supply (EU COM/2017/0490). The list of 27 CRMs features elemental groups and single elements, including platinum group metals (PGM) and REEs (EU COM/2017/0490). The REEs are divided into light REE [lanthanum (La), cerium (Ce), praseodymium (Pr), neodymium (Nd), samarium (Sm), europium (Eu)] and heavy REE [gadolinium (Gd), terbium (Tb), dysprodim (Dy), holmium (Ho), erbium (Er), thulium (Tm), ytterbium (Yb), lutetium (Lu), including yttrium (Y)] (Xu et al. 2017) plus scandium (Sc)

(Binnemans et al. 2018). Depending on the origin of the bauxite residue generated, it may be a potentially valuable source of CRM and other elements e.g. REEs, Sc, V, Ga, and titanium (Ti) (Liu and Naidu, 2014). Also included in the 2017 CRM list is P and phosphate rock, which are also of particular interest, as bauxite residue has been previously identified as having a high P retention capacity (Grace et al. 2015, 2016; Cusack et al. 2018) due to its high aluminium (Al) and iron (Fe) oxide content (IAI, 2015), making it a possible resource in the removal and recovery of P from aqueous solutions (Grace et al. 2015; Cusack et al. 2018).

Although bauxite residues are typically similar in composition, properties can vary between refineries and this is attributed to the type of ore used, as well as different process parameters, such as temperature, pressure and concentrations of caustic soda (NaOH), slaked lime (Ca(OH)₂) and other additives used in the Bayer process (Gräfe et al. 2011). This indicates that re-use options should be refinery-specific (Balomenos et al. 2017). A further potential limitation, is that bauxite residue composition, such as pH and bulk density, may change over time in storage (Kong et al. 2017a; Zhu et al. (2016a,b), which greatly influences the possibility of reusing bauxite residue.

To date, no study has investigated the CRM content variability in bauxite residue stored within one specific BRDA. Therefore, the objectives of this study were to: (1) characterise the physico-chemical, elemental and mineralogical composition of the dominant fraction (fine fraction) bauxite residue in storage over a twelve-year period, and to determine if there is any variation over the time spent in storage, which could affect possible reuse of the bauxite residue (2) create an inventory of economically interesting elements in bauxite residue over the storage period, and (3) calculate the financial value of economically interesting elements present in the bauxite residue.

2. Materials and methods

2.1. Site description and sample collection

Bauxite residue was obtained from a European refinery, who operated a separation technique to isolate the fine (particle sizes <100 µm) and coarse (particle sizes >150 µm) fractions of bauxite residue before disposal (IAI, 2015), in an approximate ratio of 9:1 (fine: coarse). Bauxite residue was sampled to a depth of 30 cm and the bulk samples were stored in 1 L containers, returned to the laboratory, and dried at 105 °C for 24 h. Once dry, the samples were pulverised using a mortar and pestle and sieved to a particle size <2 mm. In this paper, the age of the samples will be described (Table 1) relative to the sample collection time (2016).

Table 1

Sample information regarding the year of production for each of the bauxite residue samples over a twelve-year period. The sample code for each bauxite residue sample is also included in the table.

Sample Code	Sample Description	Year of Disposal
BR 12	Bauxite Residue	2004
BR 11	Bauxite Residue	2005
BR 10	Bauxite Residue	2006
BR 9	Bauxite Residue	2007
BR 8	Bauxite Residue	2008
BR 7	Bauxite Residue	2009
BR 6	Bauxite Residue	2010
BR 5	Bauxite Residue	2011
BR 4	Bauxite Residue	2012
BR 3	Bauxite Residue	2013
BR 2	Bauxite Residue	2014
BR 1	Bauxite Residue	2015

2.2. Characterisation study

2.2.1. Physico-chemical composition

The bauxite residue samples were characterised (n = 3) for their physical, chemical, elemental and mineralogical properties (Fig. 1). The pH and electrical conductivity (EC) were measured using a 5 g sample in an aqueous extract, using a 1:5 ratio (solid: liquid) (Courtney and Harrington, 2010). The bulk density (ρ_b) was determined after Blake (1965), the effective particle size analysis (PSA) was determined on particle sizes <53 µm using optical laser diffraction on a Malvern Zetasizer 3000HS[®] (Malvern, United Kingdom) with online autotitrator and a Horiba LA-920, and reported at specific cumulative % (10, 50 and 90%). Thermogravimetric analysis (TGA) was carried out to identify any change in mass over time with temperature, and change in heat flow over time with temperature was analysed using differential scanning calorimetry (DSC). TGA and DSC were carried performed using a Labsys TG (DSC/TGA 1600) in a nitrogen (N) atmosphere at a temperature range of 30 °C–1000 °C at a heating rate of 10 °C min⁻¹ (Borra et al. 2015). Due to cost limitations, only six samples were analysed (BR12, BR10, BR8, BR6, BR4 and BR2).

2.2.2. Mineralogical composition

Mineralogical detection was carried out on 1 g powdered samples using X-ray diffraction (XRD) on a Philips X'Pert PRO MPD[®] (California, USA) at 40 kV, 40 mA, 25 °C by Cu X-ray tube ($K\alpha$ -radiation). The patterns were collected in the angular range from 5 to 80° (2 θ) with a step-size of 0.008° (2 θ) (Castaldi et al. 2011), whilst surface morphology and elemental detection were carried out using scanning electron microscopy (SEM) and energy-dispersive X-ray spectroscopy (EDS) on a Hitachi SU-70 (Berkshire, UK). X-ray fluorescence (XRF) analysis was carried out onsite at the refinery using a Panalytical Axios XRF (Malvern, UK).

2.2.3. Elemental composition

Chemical analysis of minor elements was performed after aqua regia digestion (HCl: HNO₃) with a solid to liquid ration of 1:10 in a Multiwave 3000 (Rotor 8XF100) type microwave digestion system at 200 °C 1.25 MPa. After digestion, the solutions were filtered through 0.45 µm PVDF syringe filters and diluted in 1 M HNO₃ for the analysis (Ujaczki et al. 2017). The metal analysis was carried out using an Agilent Technologies 5100 inductively coupled plasma optical emission spectrometer (ICP-OES). The calibration curve was constructed using standard solutions of 100, 50, 10, 5 and 1 g L⁻¹ multi-element standard (Inorganic Ventures, Ireland) and 5, 2.5, 0.5, 0.25 and 0.05 g L⁻¹ REE standard (Inorganic Ventures, Ireland). The 1M HNO₃ solution was also used for the dilutions of the standard solutions and as a calibration blank. For the ICP-OES analysis, the following analytical lines (in nm) were used for the calculations of each of the elements: Ce 418.659, 446.021; cobalt (Co) 228.615, 230.786; Dy 353.171; Er 349.910, 369.265; Eu 397.197, 412.972, 420.504; Ga 294.363; Gd 335.048, 336.224; Ho 339.895, 345.600, 389.094; indium (In) 230.606, 352.609; La 333.749, 379.477, 408.671; Lu 261.541, 307.760; molybdenum (Mo) 202.032, 203.846, 204.598; Nd 401.224, 406.108, 410.945; Pr 390.843, 417.939; Sc 335.372, 361.383, 363.074; Sm 359.259, 360.949; Tb 350.914, 367.636; Tm 313.125, 342.508; Y 360.074, 371.029, 377.433; Yb 289.138, 328.937, 369.419; V 268.796, 292.401, 311.070 (Bridger and Knowles, 2000).

2.3. Statistical analysis

Pearson's correlation coefficients were used to determine any relationships between age of sample and sample properties (pH, EC, bulk density, particle size, mineralogical composition and

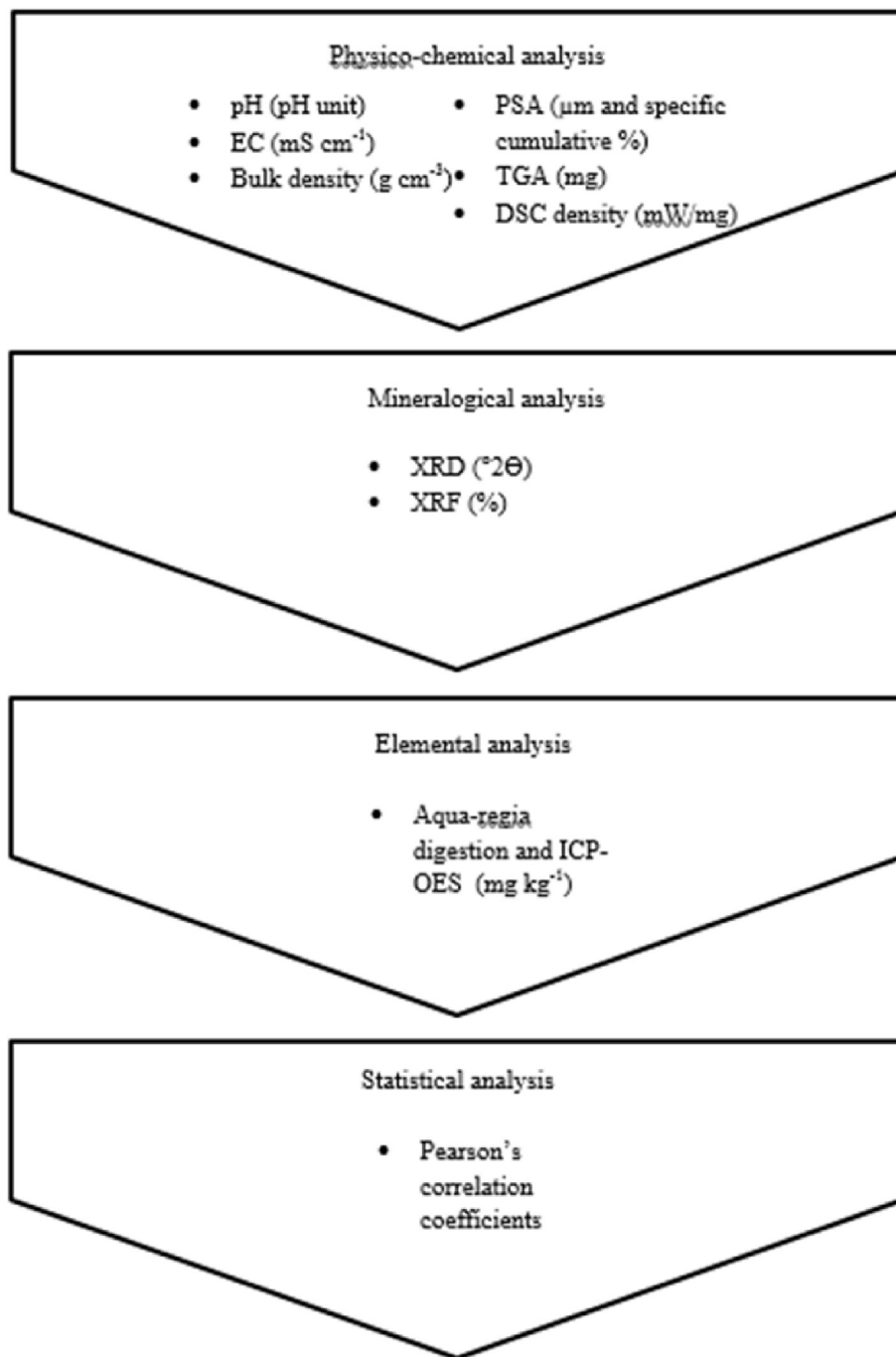


Fig. 1. Flow chart illustrating the experimental analysis carried out on the bauxite residue samples obtained. Once obtained from the BRDA, the bauxite residue was analysed for its main physico-chemical analysis (pH, EC, bulk density, PSA, TGA and DSC), mineralogical analysis (XRD and XRF), and elemental analysis (measure using ICP-OES following aqua-regia digestion). Once all data was obtained, statistical analysis was carried out using Pearson's correlation coefficients.

elemental composition), using IBM SPSS Statistics 24.

3. Results

3.1. Physico-chemical composition

The pH of the bauxite residue (Table 2) ranged from 10.0 ± 0.1 to 12.0 ± 0.02 over the twelve-year period, with the ten-year-old sample (BR10) having the highest value. The EC (Table 2) of the bauxite residue ranged from 0.4 ± 0.01 to $3.3 \pm 0.2 \text{ mS cm}^{-1}$, with again, the highest being for BR10. Small variation in the moisture

content (Table 2) for the each of the bauxite residues was recorded. The bulk density (Table 2) for the bauxite residue ranged from 1.2 ± 0.1 to $1.5 \pm 0.02 \text{ g cm}^{-3}$.

The bauxite residue had a high composition of fine particles, which ranged from 0.6 ± 0.01 to $12.7 \pm 2.3 \mu\text{m}$ (Table 2). There was some agglomerate formation evident in all samples, as seen in the accumulation of finer particles in the images captured by SEM (Figs. S1, S2, S3 in the Supplementary Information). The medium value, d_{50} , of the particle size distribution for bauxite residues ranged from $2.2 \pm 0.1 \mu\text{m}$ (BR1) to $4.3 \pm 0.4 \mu\text{m}$ (BR9). Ninety percent of the distribution (d_{90}) was under $12.7 \pm 2.7 \mu\text{m}$ and 10%

Table 2

Physico-chemical composition of the bauxite residue mud over a twelve-year storage period, inclusive of pH, EC, moisture content, bulk density and particle size distribution.

Sample	pH	EC (mS cm ⁻¹)	Moisture content (%)	Bulk density (g cm ⁻³)	d ₁₀ (μm) ^a	d ₅₀ (μm) ^b	d ₉₀ (μm) ^c
BR 12	11.6 ± 0.02	1.0 ± 0.01	26.8 ± 0.7	1.4 ± 0.04	0.7 ± 0.1	2.6 ± 0.1	7.0 ± 1.2
BR 11	10.8 ± 0.1	0.4 ± 0.02	28.2 ± 0.7	1.3 ± 0.03	0.9 ± 0.1	3.5 ± 0.5	9.6 ± 0.5
BR 10	12.0 ± 0.02	3.3 ± 0.2	26.8 ± 0.1	1.4 ± 0.1	1.4 ± 0.1	4.0 ± 0.3	12.3 ± 1.6
BR 9	10.0 ± 0.1	0.4 ± 0.01	24.3 ± 0.3	1.1 ± 0.1	1.0 ± 0.1	4.3 ± 0.4	12.4 ± 1.0
BR 8	11.4 ± 0.1	1.0 ± 0.1	27.2 ± 0.3	1.4 ± 0.1	0.8 ± 0.1	2.6 ± 0.1	6.8 ± 0.2
BR 7	10.4 ± 0.02	0.5 ± 0.01	22.3 ± 0.6	1.4 ± 0.04	0.9 ± 0.2	3.2 ± 0.5	12.7 ± 2.7
BR 6	10.7 ± 0.03	0.5 ± 0.03	25.8 ± 1.0	1.3 ± 0.04	0.7 ± 0.1	2.6 ± 0.01	6.7 ± 0.2
BR 5	10.3 ± 0.1	0.4 ± 0.03	22.0 ± 0.5	1.2 ± 0.1	0.6 ± 0.01	2.4 ± 0.04	7.9 ± 1.1
BR 4	11.5 ± 0.1	0.9 ± 0.02	31.1 ± 0.5	1.3 ± 0.1	1.2 ± 0.1	3.8 ± 0.6	12.70 ± 2.3
BR 3	10.6 ± 0.02	0.5 ± 0.01	23.8 ± 0.3	1.3 ± 0.03	0.8 ± 0.2	2.6 ± 0.3	8.3 ± 1.6
BR 2	11.2 ± 0.01	0.9 ± 0.02	28.1 ± 1.9	1.3 ± 0.1	1.1 ± 0.02	3.2 ± 0.02	9.7 ± 0.9
BR 1	10.3 ± 0.1	0.7 ± 0.03	25.0 ± 2.7	1.5 ± 0.02	0.5 ± 0.01	2.2 ± 0.1	6.7 ± 0.6

^a d₁₀ (μm) = the size of particles at 10% of the total particle distribution.^b d₅₀ (μm) = the median; the size of particles at 50% of the total particle distribution.^c d₉₀ (μm) = the size of particles at 90% of the total particle distribution.

(d₁₀) was under 0.5 ± 0.01 μm (Table 2). Iron, Al, sodium (Na), calcium (Ca), titanium (Ti), and silicon (Si) were the main elements present in all the bauxite residue samples (Fig. S4). TGA curves showed weight loss between 300 and 975 °C for all the bauxite residues (Fig. 2 and S5). However, sample BR12 (from 2014) had a larger temperature range over which weight loss occurred (between 150 and 975 °C).

3.1.1. Mineralogical composition

The main mineralogical composition of the bauxite residue detected by XRD included haematite (Fe₂O₃), goethite (FeO(OH)), perovskite (CaTiO₃), rutile (TiO₂), gibbsite Al(OH)₃, sodalite (Na₈(Al₆Si₆O₂₄)Cl₂) and cancrinite (Na₆Ca₂(CO₃)) (Figs. S6 and S7). Sample BR9 had an extra rutile peak at position 27.459 °2θ and no sodalite peak at position 14 °2θ; samples BR1 to BR6 had similar patterns, but with less intense peaks and sodalite peaks at position 14 °2θ (Fig. S6). Sample BR1 had one peak of boehmite (AlO(OH)) at position 13.9 °2θ and gibbsite at position 18.5 °2θ (Fig. S6). Sample BR1 also had an unidentified peak at position 47 °2θ (Fig. S6).

XRF analysis carried out on the bauxite residue samples (Table 3) reflected the main mineralogical composition detected by XRD analysis. The dominant oxides found were Fe₂O (ranging from 40.1 ± 1.40 to 47.5 ± 2.0%) and Al₂O₃ (14.8 ± 1.5 to 17.8 ± 0.73%). SiO₂ (7.20 ± 1.0 to 10.9 ± 0.47%), TiO₂ (8.62 ± 0.71 to 10.3 ± 0.95%) and CaO (5.70 ± 0.66 to 6.1 ± 1.0%) were also present (Table 3).

3.1.2. Elements of economic importance in bauxite residue

An extensive inventory of CRMs and further elements of economic importance were developed using microwave-assisted aqua

Table 3

Main mineralogical composition (%) of the bauxite residue samples taken from the BRDA ranging from one to twelve years old, as determined by XRF.

Code	Al ₂ O ₃	Fe ₂ O	SiO ₂	TiO ₂	CaO
BR 11	17.0 ± 0.61	42.0 ± 1.20	9.82 ± 0.32	9.41 ± 0.34	6.03 ± 0.79
BR 10	17.1 ± 0.4	41.5 ± 0.96	10.2 ± 0.56	9.52 ± 0.6	6.03 ± 0.49
BR 9	17.8 ± 0.73	40.1 ± 1.40	10.9 ± 0.47	8.97 ± 0.51	6.04 ± 0.4
BR 8	16.8 ± 0.58	41.8 ± 1.40	9.89 ± 0.39	9.41 ± 0.61	5.97 ± 0.49
BR 7	14.8 ± 1.5	47.5 ± 2.0	7.20 ± 1.0	10.3 ± 0.95	6.1 ± 1.0
BR 6	16.2 ± 0.54	45.9 ± 2.10	8.0 ± 0.57	9.54 ± 0.78	5.70 ± 0.66
BR 5	16.2 ± 0.66	44.4 ± 1.30	9.35 ± 0.60	8.62 ± 0.71	5.75 ± 0.53
BR 4	16.5 ± 0.65	43.3 ± 1.20	9.38 ± 0.53	8.91 ± 0.53	6.21 ± 0.35
BR 3	15.8 ± 0.45	44.3 ± 1.90	8.85 ± 0.47	9.18 ± 0.62	6.34 ± 0.35
BR 2	16.0 ± 0.71	46.6 ± 1.80	8.95 ± 0.70	8.21 ± 0.38	5.0 ± 0.40
BR 1	16.2 ± 0.6	46.8 ± 1.61	8.76 ± 0.48	8.33 ± 0.56	4.69 ± 0.43

regia digestion, with subsequent ICP-OES analysis (Table 4). Overall, no trend was noted in the elemental content between the oldest and newest bauxite residue in the BRDA. However, In, Mo, Ce, Nd, Dy and Er were present in smaller amounts in the oldest samples compared to the fresh sample. Terbium (Tb), Tm and Ho were not detected in the bauxite residue.

4. Discussion

4.1. Characterisation of bauxite residue

Bauxite residue typically has a pH > 10 (Goloran et al. 2013) and an EC ranging from 1.4 to 28.4 mS cm⁻¹ (Gräfe et al. 2011). The high

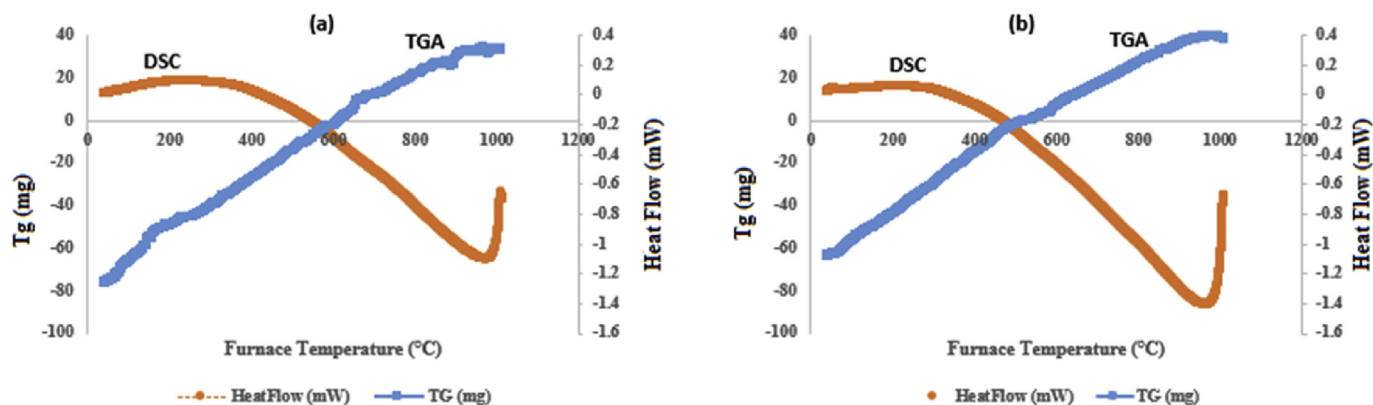


Fig. 2. TGA (descending)/DSC (ascending) curve obtained for bauxite residue (a) BR12 (2004) and (b) BR2 (2014). Remaining TGA/DSC graphs found in Fig. S4. The TGA curves showed weight loss between 300 and 975 °C for all the bauxite residues examined.

Table 4
CRM composition (in mg kg⁻¹) of the bauxite residue samples, taken from the BRDA, as detected on ICP-OES following aqua regia digestion.

Element	BR 12	BR 11	BR 10	BR 9	BR 8	BR 7	BR 6	BR 5	BR 4	BR 3	BR 2
Dy	3.6 ± 0.02	5.4 ± 0.01	7.19 ± 0.01	5.39 ± 0.001	5.4 ± 0.04	5.39 ± 0.01	5.4 ± 0.01	5.38 ± 0.02	4.51 ± 1.3	7.2 ± 0.002	5.4 ± 0.02
Er	4.8 ± 0.5	5.4 ± 0.01	5.7 ± 0.5	4.94 ± 0.6	5.4 ± 0.04	5.39 ± 0.01	4.49 ± 0.01	5.38 ± 0.01	4.05 ± 0.6	5.4 ± 0.001	5.4 ± 0.02
Lu	8.39 ± 0.5	7.8 ± 0.5	8.09 ± 0.01	7.49 ± 0.5	8.1 ± 0.05	7.63 ± 0.6	8.1 ± 0.02	8.37 ± 0.5	7.66 ± 0.7	8.1 ± 0.002	8.09 ± 0.03
Y	35.6 ± 3.2	39.8 ± 1.2	44.4 ± 1.5	41.9 ± 1.5	42 ± 0.4	39.5 ± 0.04	33.4 ± 0.4	41 ± 2.0	36.9 ± 1.4	47.4 ± 1.2	39.3 ± 0.5
Yb	8.39 ± 0.6	8.8 ± 0.3	9.39 ± 0.3	8.79 ± 0.7	9.4 ± 0.3	8.68 ± 0.4	8.2 ± 0.4	8.97 ± 0.9	8.11 ± 0.4	9.6 ± 0.002	8.71 ± 0.4
Ce	126 ± 10.1	126 ± 3.5	156 ± 2.2	136 ± 7.6	157 ± 2.2	128 ± 3.3	146 ± 6.7	200 ± 8.4	102 ± 3.5	147 ± 4.2	139 ± 6.8
Eu	2.40 ± 0.01	2.40 ± 0.01	2.40 ± 0.005	2.40 ± 0.01	2.40 ± 0.02	2.39 ± 0.003	2.40 ± 0.01	3.59 ± 0.01	2.40 ± 0.01	2.40 ± 0.001	2.40 ± 0.005
Gd	6.75 ± 0.6	6.60 ± 0.5	7.64 ± 0.6	7.63 ± 0.6	9.30 ± 0.6	7.18 ± 1.3	6.75 ± 0.6	8.98 ± 0.02	5.41 ± 0.02	9 ± 0.002	6.73 ± 0.6
La	91.3 ± 8.6	88.2 ± 3.2	108 ± 2.3	94.1 ± 2.7	106.4 ± 1.0	89.2 ± 0.9	104 ± 3.5	134 ± 4.4	68.8 ± 4.0	98.2 ± 2.1	91 ± 2.4
Nd	80.1 ± 7.4	77.2 ± 5.3	93.9 ± 6.5	84.7 ± 1.3	98 ± 5.3	85.6 ± 8.6	88.9 ± 8.6	118 ± 4.4	64.6 ± 4.0	93 ± 2.2	94.3 ± 11.3
Pr	41.1 ± 3.5	42.9 ± 4.2	47.7 ± 3.3	42.5 ± 3.1	50.1 ± 1.6	40.8 ± 1.9	45 ± 2.7	56.2 ± 5.3	34.7 ± 3.3	45 ± 0.9	42.3 ± 1.1
Sc	50.2 ± 4.1	50.4 ± 1.6	60.2 ± 2.2	56.1 ± 2.7	54.2 ± 0.9	55.7 ± 1.3	45.4 ± 0.2	56 ± 4.2	42.9 ± 2.3	49 ± 1.3	45.6 ± 4.3
Sm	19.3 ± 0.7	20.7 ± 1.8	21 ± 2.2	21.6 ± 0.9	21.6 ± 0.8	18.4 ± 1.9	21.6 ± 0.9	25.1 ± 0.05	18 ± 1.2	21 ± 1.0	20.3 ± 2.0
Co	8.69 ± 0.5	7.64 ± 0.6	7.79 ± 0.5	6.73 ± 0.6	8.10 ± 0.05	7.63 ± 0.6	6.6 ± 0.5	8.67 ± 0.5	7.21 ± 0.02	8.4 ± 0.5	7.49 ± 0.6
Ga	107 ± 8.5	112 ± 2.3	102 ± 0.7	114 ± 5.2	98.6 ± 0.2	113 ± 3.8	106 ± 2.7	114 ± 5.1	99.5 ± 1.8	114 ± 1.9	94.4 ± 2.7
In	30.1 ± 1.8	34.6 ± 0.7	31.5 ± 1.5	32.1 ± 2.7	36.9 ± 0.9	30.5 ± 1.3	29.2 ± 2	33.6 ± 0.7	28.4 ± 0.7	34.5 ± 7.2	36.4 ± 4.3
Mo	3.14 ± 0.6	4.49 ± 0.01	4.04 ± 0.6	4.95 ± 0.6	4.48 ± 0.004	4.95 ± 0.6	4.49 ± 0.01	4.48 ± 0.01	4.94 ± 1.9	4.8 ± 0.5	4.48 ± 0.01
V	593 ± 60.6	419 ± 8.2	596 ± 19.8	439 ± 41.1	491 ± 20.3	445 ± 41.2	484 ± 48.2	600 ± 24.3	401 ± 41.2	571 ± 13.3	573 ± 41.1

pH is attributed to the presence of alkaline anions such as hydroxides (OH⁻), carbonate or bicarbonates (CO₃²⁻/HCO₃⁻), aluminates or aluminium hydroxides (Al(OH)₄/Al(OH)₃), and di/trihydrogen orthosilicates (H₂SiO₄²⁻/H₃SiO₄⁻) introduced and formed during the Bayer process (Gräfe et al. 2011). At the end of the Bayer process, prior to disposal, residue undergoes a repeated washing stage. However, the bauxite residue remains highly alkaline due to the alkalinity being in the form of slow dissolving solid phases (Gräfe et al. 2011).

Depending on the refinery and the advances in residue management steps employed, the pH may be further reduced through practices such as atmospheric carbonation (mud farming) (Clohessy, 2015; Evans, 2016), seawater disposal (Menzies et al. 2009), application of spent acid (Kirwan et al. 2013), phosphogypsum (Xue et al. 2018), or by the addition of an acidic gas such as CO₂ or SO₂ (Xue et al. 2016). Consequently, surface pH values for residues may vary between refineries and within BRDAs.

The bauxite residue examined in this study showed variation in terms of both the pH and the EC ($p < 0.01$) (Table 2). Whilst the pH and EC did decrease across all the bauxite residue samples examined in this study (Table 2), this was attributed to different causes. The reduced pH value of the fresh bauxite residue examined (BR1) in this study (Table 2) is as a result of the atmospheric carbonation technique, mud farming, which can effectively decrease alkalinity (Clohessy, 2015; McMahan, 2017). This helps in removing the alkalinity limitation/barrier to the reutilisation of the bauxite residue (Evans, 2016) and has been shown to successfully decrease the pH of fresh bauxite residue (~13.5) to below < 11.5 within seven days (Clohessy, 2015). The mud farming technique sequesters CO₂ from the atmosphere, allowing for the accelerated carbonation of the bauxite residue (IAI, 2015; Evans, 2016). Due to this process, the free OH⁻ present in the bauxite residue is neutralised due to the carbonation of the CO₂ present in the surrounding atmosphere (air), resulting in the formation of carbonates, therefore creating a buffering effect, which results in a drop in pH (Han et al. 2017).

Natural weathering processes may play an important role in the improvement of the physico-chemical composition of bauxite residue in storage (Zhu et al. 2018). The reduction observed in the pH of the older samples (Table 2) is as a result of the natural ageing and weathering of the bauxite residue in storage. Evidence of the natural weathering decreasing the pH was shown by Khaïtan et al. (2010), who reported a pH of 10.5 for 14-year-old bauxite residue and 9.5 for 35-year-old bauxite residue, with the decreases attributed to the slow carbonation from atmospheric CO₂. Zhu et al.

(2016a,b) also measured a decrease in residue pH from 10.98 to 9.45 in stored bauxite residue exposed to natural weathering processes. Similar to pH, EC usually decreases with time in the storage area due to weathering (Zhu et al. 2016a; b; Kong et al. 2017a). Rainfall events allow the soluble alkaline minerals such as sodalite and calcite, which result in a buffering effect for both pH and salinity (EC) (Santini and Fey, 2013).

The thermal analysis (TGA/DSC) indicated an overall weight loss occurring between 300 and 975 °C for all the bauxite residue samples examined. Previous work has shown weight loss between temperature ranges of 300 and 600 °C (attributed to the decomposition of hydroxides in different stages), 300 and 400 °C (as a result of the decomposition of diaspora), and between 600 and 800 °C (due to the decomposition of calcium carbonate) (Agatzini-Leonardou et al. 2008), all dominant minerals in bauxite residue. There were numerous endothermic peaks observed on the DSC curve for the six samples examined, particularly in the region above 800 °C. Endothermic peaks above this temperature are indicative of the decomposition of sodalite phases and also the decomposition of quartz, which occurs between 550 and 1000 °C (Atasoy, 2005). Small endothermic peaks throughout the DSC curve may be attributed to loss of physically held water (Atasoy, 2005), which was notable in all the bauxite residue samples examined.

The mineralogical composition of bauxite residue typically comprises Al₂O₃ and Fe₂O₃ in the range of 20–45% and 10–22%, respectively (IAI, 2015). This composition is reflected in the XRF and XRD analysis, which showed the dominant presence of Fe₂O₃, FeO(OH), and Al(OH)₃. CaTiO₃, AlO(OH) and TiO₂ were also detected in all samples, which is common amongst bauxite residue (Gräfe et al. 2011). Sodalite (Na₈(Al₆Si₆O₂₄)Cl₂) was also present in the bauxite residue, and is one of the most common desilication products formed during the pre-desilication stage during the Bayer process, along with CaTiO₃ which is often found as a result of the lime added (Gräfe et al. 2011).

4.2. Economic value of bauxite and potential for reuse

In recent years, several studies have been conducted to investigate the potential use of industrial residues such as phosphogypsum, mine tailings, slags and bauxite residue as a possible source for CRMs and REEs (Binnemans et al. 2015). Currently, the global production rate of REEs, which is typically expressed in tons of rare earth oxides (REOs) is 130,000 to 140,000 tons, of which 95% is produced in China (Binnemans et al. 2018). Five of the REEs (Nd,

Table 5

Associated financial value of economically interesting elements in the bauxite residue (average over a twelve-year period, n = 11).

Element	Average aqua regia extracted content (mg kg ⁻¹)	Price ^a (US \$ t ⁻¹)	Economic value of the bauxite residue in this study ^c (US \$ t ⁻¹)
Ga	107 ± 7.3	400,000	42.73
Sc	51.4 ± 5.4	4,600,000	236.44
In	32.5 ± 2.9	240,000	7.81
V	510 ± 77.8	6889	3.51
Nd	89.0 ± 13.6	39,500	3.51
Dy	5.48 ± 1.0	184,500	1.01
Pr	44.4 ± 5.6	5,500 ^b	0.24
Y	40.1 ± 3.9	35,500	1.42
Ce	142 ± 24.9	2000	0.28
Sm	20.8 ± 1.9	12,500 ^b	0.26
Co	7.72 ± 0.7	26,444	0.20
La	97.5 ± 16.3	2000	0.19
Eu	2.51 ± 0.4	66,000	0.16
Yb	8.82 ± 0.5	5,500 ^b	0.04
Lu	7.99 ± 0.3	5,500 ^b	0.04
Gd	7.45 ± 1.2	5,500 ^b	0.04
Mo	4.48 ± 0.5	14,500	0.06
Er	5.12 ± 0.5	5,500 ^b	0.03

^a Values from USGS (2016).^b Average value for mischmetals of REE/expected higher individual prices.^c Economic value of the bauxite residue in this study, determined using current price (US \$ t⁻¹) and the average content in the bauxite residue studied.

Eu, Tb, Dy, Y) are now described as being of a high supply risk within Europe, Japan and the USA (Binnemans et al. 2018). Such CRMs and REEs are necessary for the production of magnets, lighting, lasers, batteries, catalysts, and alloys in aerospace (Weng et al. 2015).

While this study did show differences in the bauxite residue over the twelve-year period, in terms of decreased pH and EC, there were no significant changes in the CRM content of the bauxite residue (Table 4). This indicates that some BRDAs may be a potential resource for the reprocessing and recovery of CRMs and REEs. However, this is not certain for all BRDAs, as variation can and does occur within BRDAs and refineries due to differences in bauxite ore type, parameters used within the Bayer Process, as well as varying disposal and neutralisation techniques.

The Sc, Ga and V content of the bauxite residue in the current study are of particular interest, due to their high economic value (Table 5) and supply risk. Scandium, a trace constituent of igneous rocks (European Commission, 2017), is used in the production of aluminium alloys (Ricketts and Duyvesteyn, 2018), and V, present in minor amounts in the Earth's crust and seawater and the majority of which is sourced as a by-product of the steel industry (European Commission, 2017), is used in electrodes (Morel et al. 2016). Gallium is primarily sourced from bauxite ore and bauxite residue, as it found naturally as a trace element dispersed in minerals, which also includes coal (Qin et al. 2015), and is used in the production of catalysts (Qin and Schneider, 2016). The Sc in this study (Table 4) was lower than values found in fresh Hungarian (Ujaczki et al. 2017), Greek (Borra et al. 2015), Russian (Petrakova et al. 2015) and Australian (Wang et al. 2013) bauxite residues. However, the Ga content (Table 4) was higher than that found by Ujaczki et al. (2017) in Hungarian bauxite residue, as well as in Australian (Wang et al. 2013), Indian (Mohapatra et al. 2012) and Turkish (Abdulvaliyev et al. 2015) bauxite residues. Finally, the V content was present in higher amounts compared to Hungarian (Ujaczki et al. 2017), Indian (Mohapatra et al. 2012) and Turkish (Abdulvaliyev et al. 2015) bauxite residues. This is indicative of the variation of CRM content in residues between refineries. In addition to Sc, Ga and V, there is now a focus on further valuable element extraction (Jowitt et al. 2018) and recovery of REE due to the overproduction of REEs such as La and Ce, which is leading to an imbalance in the supply of REEs produced and a demand for Nd and Dy (Binnemans and Jones, 2015; Binnemans et al. 2018), both of

which were found in the bauxite residue in this study.

The typical methods of CRM recovery from bauxite residue include direct leaching using mineral acids such as HNO₃, sulphuric acid (H₂SO₄) or hydrochloric acid (HCl), or leaching following pyrometallurgical applications such as roasting (Ujaczki et al. 2018). Although there are high recovery rates of CRMs from bauxite residue reported (Abdulvaliyev et al. 2015; Borra et al. 2015), so too are the associated costs for acids and energy required in these processes, which questions the justification of extracting CRMs from by-products such as bauxite residue. Recent studies have also highlighted the need to develop new technologies to optimise the efficiency of CRM recovery from bauxite residue to ensure cost-effectiveness (Gomes et al. 2016; Akcil et al. 2018). Ujaczki et al. (2018) in their review on the reuse of bauxite residue as a source of CRMs, highlighted the extent of the benefits following CRM recovery from a wider perspective in terms of the technological (development of more efficient technologies), social (such as improvements to health), economic (mainly reduction in refinery disposal costs), and environmental factors such as reduced emissions and loss of habitable land.

4.3. The findings of this study from an industrial perspective on potential re-use of bauxite residue

This study found that there was very little variation in the CRM content of bauxite residue in a BRDA over a twelve-year period. This shows promise for the potential reuse of bauxite residue as a secondary source of CRMs. Finding a suitable and long-term use for bauxite residue may be hampered by several barriers and limitations (Klauber et al. 2011; Evans, 2016), such as high alkalinity and salinity which were shown by this study to be reduced by weathering and mud farming. However, limitations to the reuse of bauxite residue may be overcome through management strategies involving its partial neutralisation and increased solids content (Klauber et al. 2011).

5. Conclusions

This study showed that there was a reduction in both the pH and the EC ($p < 0.01$) of bauxite residue in a BRDA over a twelve-year period. There was little variation in the CRM content of the bauxite residue sampled. The CRMs of particular interest were V, Ga

and Sc due their potential supply risk and associated economic value. The V, Ga and Sc content of the bauxite residue samples were 510 ± 77.8 , 107 ± 7.3 and 51.4 ± 5.4 mg kg⁻¹, respectively, giving current economic values of 3.51, 42.73 and 236.44 US \$ t⁻¹. From a European and global context, this highlights a potential resource for CRMs in the event of a scarcity of these materials. However, the general composition and CRM content of bauxite residue varies greatly due to the bauxite ore and parameters used in the Bayer Process, as well as the disposal and neutralisation methods implemented by refineries. Depending on the history of the refinery and BRDA, there may be little variation over time, making BRDAs possible sources for the extraction of CRMs. There are currently high-costs associated with the extraction of CRMs from bauxite residue due to the large amount of reagent and/or energy required in the process, before purifying the CRMs recovered for reuse. However, these need to be set against the overall benefits of recovering CRMs in terms of the environmental, economic and social factors. Further research is necessary to investigate the cost and environmental implications and limitations of extraction of CRMs from BRDAs, as opposed to conventional extraction techniques from mines, in terms of emissions produced, machinery required, fuel needed and human resources required.

Acknowledgements

The authors would like to acknowledge the financial support of the Environmental Protection Agency (EPA) (2014-RE-MS-1).

Appendix A. Supplementary data

Supplementary data to this article can be found online at <https://doi.org/10.1016/j.jclepro.2018.10.083>.

References

- Abdulvaliyev, R.A., Akcil, A., Gladyshev, S.V., Tastanov, E.A., Beisembekova, K.O., Akhmediyeva, N.K., Devci, H., 2015. Gallium and vanadium extraction from red mud of Turkish alumina refinery plant: hydrogarnet process. *Hydrometallurgy* 157, 72–77.
- Agatzini-Leonardou, S., Oustadakis, P., Tsakiridis, P.E., Markopoulos, C., 2008. Titanium leaching from red mud by diluted sulfuric acid at atmospheric pressure. *J. Hazard Mater.* 157, 579–586.
- Akcil, A., Akhmediyeva, N., Abdulvaliyev, R., Abhilash, Meshram, P., 2018. Overview on extraction and separation of rare earth elements from red mud: focus on scandium. *Miner. Process. Extr. Metall. Rev.* 39, 145–151.
- Arco-Lázaro, E., Pardo, T., Clemente, R., Bernal, M.P., 2018. Arsenic adsorption and plant availability in an agricultural soil irrigated with As-rich water: effects of Fe-rich amendments and organic and inorganic fertilisers. *J. Environ. Manag.* 209, 262–272.
- Atasoy, A., 2005. An investigation on characterization and thermal analysis of the Aughinish red mud. *J. Therm. Anal. Calorim.* 81, 357–361.
- Atasoy, A.D., Bilgic, B., 2018. Adsorption of copper and zinc ions from aqueous solutions using montmorillonite and bauxite as low-cost adsorbents. *Mine Water Environ.* 37, 205–210.
- Balomenos, E., Davris, P., Pontikes, Y., Panias, D., 2017. Mud2Metal: lessons learned on the path for complete utilization of bauxite residue through industrial symbiosis. *J. Sustain. Metall.* 3, 551–560.
- Bhatnagar, A., Vilar, V.J., Botelho, C.M., Boaventura, R.A., 2011. A review of the use of red mud as adsorbent for the removal of toxic pollutants from water and wastewater. *Environ. Technol.* 32, 231–249.
- Binnemans, K., Jones, P.T., 2015. Rare earths and the balance problem. *J. Sustain. Metall.* 1, 29–38.
- Binnemans, K., Jones, P.T., Blanpain, B., Van Gerven, T., Pontikes, Y., 2015. Towards zero-waste valorisation of rare-earth-containing industrial process residues: a critical review. *J. Clean. Prod.* 99, 17–38.
- Binnemans, K., Jones, P.T., Müller, T., Yurramendi, L., 2018. Rare earths and the balance problem: how to deal with changing markets? *J. Sustain. Metall.* 4, 1–21.
- Blake, G.R., 1965. Bulk Density 1. *Methods of Soil Analysis. Part 1. Physical and Mineralogical Properties, Including Statistics of Measurement and Sampling, (Methodsofsoilana)*, pp. 374–390. Available: <https://dl.sciencesocieties.org/publications/books/tocs/agronomymonogra/methodsofsoilana>. (Accessed 24 May 2018).
- Borra, C.R., Pontikes, Y., Binnemans, K., Van Gerven, T., 2015. Leaching of rare earths from bauxite residue (red mud). *Miner. Eng.* 76, 20–27.
- Bridger, S., Knowles, M., 2000. A Complete Method for Environmental Samples by Simultaneous Axially Viewed ICP-AES Following USEPA Guidelines. Varian ICP-OES at Work (29). Available: <https://www.agilent.com/cs/library/applications/ICPES-29.pdf>. (Accessed 24 May 2018).
- Burke, I.T., Peacock, C.L., Lockwood, C.L., Stewart, D.I., Mortimer, R.J., Ward, M.B., Renforth, P., Gruiz, K., Mayes, W.M., 2013. Behavior of aluminum, arsenic, and vanadium during the neutralization of red mud leachate by HCl, gypsum, or seawater. *Environ. Sci. Technol.* 47, 6527–6535.
- Castaldi, P., Silvetti, M., Enzo, S., Deiana, S., 2011. X-ray diffraction and thermal analysis of bauxite ore-processing waste (red mud) exchanged with arsenate and phosphate. *Clay Clay Miner.* 59, 189–199.
- Clohesy, J., 2015. Closure and rehabilitation of rural aughinish BRDA, presented at the residue closure and rehabilitation workshop. In: In 10th Alumina Quality Workshop, Perth, Western Australia. Available: <http://aqw.com.au/2015papers.html>. (Accessed 18 April 2018).
- Cooling, D.J., 2007. Improving the Sustainability of Residue Management Practices—Alcoa World Alumina Australia. Paste and Thickened Tailings: a Guide, p. 316. Available: <http://citeseerx.ist.psu.edu/viewdoc/download?doi=10.1.1.629.1067&rep=rep1&type=pdf>. (Accessed 24 May 2018).
- Courtney, R., Harrington, T., 2010. Assessment of plant-available phosphorus in a fine textured sodic substrate. *Ecol. Eng.* 36, 542–547.
- Cusack, P.B., Healy, M.G., Ryan, P.C., Burke, I.T., O'Donoghue, L.M., Ujaczki, E., Courtney, R., 2018. Enhancement of bauxite residue as a low-cost adsorbent for phosphorus in aqueous solution, using seawater and gypsum treatments. *J. Clean. Prod.* 179, 217–224.
- Dursun, S., Guclu, D., Berkay, A., Guner, T., 2008. Removal of chromate from aqueous system by activated red-mud. *Asian J. Chem.* 20, 6473–6478.
- EU, 2000. Communities Commission Decision 2000/532/EC, OJ L 226, 06.09, pp. 3–24. Available online: <http://eur-lex.europa.eu/legal-content/EN/TXT/PDF/?uri=CELEX:22002D0009&from=EN>. (Accessed 27 September 2018).
- EU, 1999. Communities Council Directive 1999/31/EC on the Landfill of Waste, OJ L 182, 16.07, pp. 1–19. Available online: <http://eur-lex.europa.eu/legal-content/EN/TXT/PDF/?uri=CELEX:31999L0031&from=EN>. (Accessed 27 September 2018).
- European Commission, 2017. Study on the Review of the List of Critical Raw Materials. Critical Raw Materials Factsheets. Catalogue number ET-04-15-307-EN-N. Available: <https://publications.europa.eu/en/publication-detail/-/publication/7345e3e8-98fc-11e7-b92d-01aa75ed71a1/language-en>. (Accessed 15 May 2018).
- Evans, K., 2016. The history, challenges, and new developments in the management and use of bauxite residue. *J. Sustain. Metall.* 2, 316–331.
- Goloran, J.B., Chen, C.R., Phillips, I.R., Xu, Z.H., Condon, L.M., 2013. Selecting a nitrogen availability index for understanding plant nutrient dynamics in rehabilitated bauxite-processing residue sand. *Ecol. Eng.* 58, 228–237.
- Gomes, H.I., Jones, A., Rogerson, M., Burke, I.T., Mayes, W.M., 2016. Vanadium removal and recovery from bauxite residue leachates by ion exchange. *Environ. Sci. Pollut. Res.* 23, 23034–23042.
- Grace, M.A., Healy, M.G., Clifford, E., 2015. Use of industrial by-products and natural media to adsorb nutrients, metals and organic carbon from drinking water. *Sci. Total Environ.* 518, 491–497.
- Grace, M.A., Clifford, E., Healy, M.G., 2016. The potential for the use of waste products from a variety of sectors in water treatment processes. *J. Clean. Prod.* 137, 788–802.
- Gräfe, M., Power, G., Klauber, C., 2011. Bauxite residue issues: III. Alkalinity and associated chemistry. *Hydrometallurgy* 108, 60–79.
- Ha, X.L., Hoang, N.H., Nguyen, T.T.N., Nguyen, T.T., Nguyen, T.H., Dang, V.T., Nguyen, N.H., 2017. October. Removal of Cd (II) from aqueous solutions using red mud/graphene composite. In: *Congrès International de Géotechnique—Ouvrages—Structures*. Springer, Singapore, pp. 1044–1052.
- Han, Y.S., Ji, S., Lee, P.K., Oh, C., 2017. Bauxite residue neutralization with simultaneous mineral carbonation using atmospheric CO₂. *J. Hazard Mater.* 326, 87–93.
- Hannachi, Y., Shapovalov, N.A., Hannachi, A., 2010. Adsorption of nickel from aqueous solution by the use of low-cost adsorbents. *Kor. J. Chem. Eng.* 27, 152–158.
- Hertel, T., Blanpain, B., Pontikes, Y., 2016. A proposal for a 100% use of bauxite residue towards inorganic polymer mortar. *J. Sustain. Metall.* 2, 394–404.
- Higgins, D., Curtin, T., Pawlett, M., Courtney, R., 2016. The potential for constructed wetlands to treat alkaline bauxite-residue leachate: phragmites australis growth. *Environ. Sci. Pollut. Res.* 23, 24305–24315.
- Higgins, D., Curtin, T., Courtney, R., 2017. Effectiveness of a constructed wetland for treating alkaline bauxite residue leachate: a 1-year field study. *Environ. Sci. Pollut. Res.* 24, 8516–8524.
- IAI, 2015. Bauxite Residue Management: Best Practice. http://www.world-aluminium.org/media/filer_public/2015/10/15/bauxite_residue_management_-_best_practice_english_oct15edit.pdf. (Accessed 14 October 2017).
- Jones, B.E., Haynes, R.J., Phillips, I.R., 2012. Addition of an organic amendment and/or residue mud to bauxite residue sand in order to improve its properties as a growth medium. *J. Environ. Manag.* 95, 29–38.
- Jowitt, S.M., Werner, T.T., Weng, Z., Mudd, G.M., 2018. Recycling of the rare Earth elements. *Curr. Opin. Green. Sustain. Chem.* 13, 1–7.
- Khaitan, S., Dzombak, D.A., Swallow, P., Schmidt, K., Fu, J., Lowry, G.V., 2010. Field evaluation of bauxite residue neutralization by carbon dioxide, vegetation, and organic amendments. *J. Environ. Eng.* 136, 1045–1053.

- Kirwan, L.J., Hartshorn, A., McMonagle, J.B., Fleming, L., Funnell, D., 2013. Chemistry of bauxite residue neutralisation and aspects to implementation. *Int. J. Miner. Process.* 119, 40–50.
- Klauber, C., Gräfe, M., Power, G., 2011. Bauxite residue issues: II. Options for residue utilization. *Hydrometallurgy* 108, 11–32.
- Kong, X., Guo, Y., Xue, S., Hartley, W., Wu, C., Ye, Y., Cheng, Q., 2017a. Natural evolution of alkaline characteristics in bauxite residue. *J. Clean. Prod.* 143, 224–230.
- Kong, X., Li, M., Xue, S., Hartley, W., Chen, C., Wu, C., Li, X., Li, Y., 2017b. Acid transformation of bauxite residue: conversion of its alkaline characteristics. *J. Hazard Mater.* 324, 382–390.
- Liu, Y., Naidu, R., 2014. Hidden values in bauxite residue (red mud): recovery of metals. *Waste Manag.* 34, 2662–2673.
- Menzies, N.W., Fulton, I.M., Kopittke, R.A., Kopittke, P.M., 2009. Fresh water leaching of alkaline bauxite residue after sea water neutralization. *J. Environ. Qual.* 38, 2050–2057.
- McMahon, K., 2017. Bauxite residue disposal area rehabilitation. In: ISCOBA Conference November 2017, Hamburg, 02–05 Oct, Hamburg, Germany. Available: <http://icsoba.org/sites/default/files/2017papers/Bauxite%20Residue%20Papers/BR01%20-%20Bauxite%20Residue%20Disposal%20Area%20Rehabilitation.pdf>. (Accessed 21 February 2018).
- Mohapatra, B.K., Mishra, B.K., Mishra, C.R., 2012. Studies on metal flow from khondalite to bauxite to alumina and rejects from an alumina refinery, India. In: *Light Metals 2012*. Springer, Cham, pp. 87–91.
- Morel, A., Borjon-Piron, Y., Porto, R.L., Brousse, T., Bélanger, D., 2016. Suitable conditions for the use of vanadium nitride as an electrode for electrochemical capacitor. *J. Electrochem. Soc.* 163, A1077–A1082.
- Nikbin, I.M., Alighazadeh, M., Charkhtab, S., Fathollahpour, A., 2018. Environmental impacts and mechanical properties of lightweight concrete containing bauxite residue (red mud). *J. Clean. Prod.* 172, 2683–2694.
- Petrakova, O.V., Panov, A.V., Gorbachev, S.N., Klimentenok, G.N., Perestoronin, A.V., Vishnyakov, S.E., Anashkin, V.S., 2015. Improved efficiency of red mud processing through scandium oxide recovery. In: *Light Metals 2015*. Springer, Cham, pp. 93–96.
- Pontikes, Y., Rathossi, C., Nikolopoulos, P., Angelopoulos, G.N., Jayaseelan, D.D., Lee, W.E., 2009. Effect of firing temperature and atmosphere on sintering of ceramics made from Bayer process bauxite residue. *Ceram. Int.* 35, 401–407.
- Pontikes, Y., Angelopoulos, G.N., 2013. Bauxite residue in cement and cementitious applications: current status and a possible way forward. *Resour. Conserv. Recycl.* 73, 53–63.
- Power, G., Gräfe, M., Klauber, C., 2011. Bauxite residue issues: I. current management, disposal and storage practices. *Hydrometallurgy* 108, 33–45.
- Qin, S., Sun, Y., Li, Y., Wang, J., Zhao, C., Gao, K., 2015. Coal deposits as promising alternative sources for gallium. *Earth Sci. Rev.* 150, 95–101.
- Qin, B., Schneider, U., 2016. Catalytic use of elemental gallium for carbon–carbon bond formation. *J. Am. Chem. Soc.* 138, 13119–13122.
- Ricketts, N.J., Duyvesteyn, W.P., 2018. March. Scandium recovery from the Nyngan laterite project in NSW. In: *TMS Annual Meeting & Exhibition*. Springer, Cham, pp. 1539–1543.
- Santini, T.C., Fey, M.V., 2013. Spontaneous vegetation encroachment upon bauxite residue (red mud) as an indicator and facilitator of in situ remediation processes. *Environ. Sci. Technol.* 47, 12089–12096.
- Tsakiridis, P.E., Agatzini-Leonardou, S., Oustadakis, P., 2004. Red mud addition in the raw meal for the production of Portland cement clinker. *J. Hazard Mater.* 116, 103–110.
- Ujaczki, É., Klebercz, O., Feigl, V., Molnár, M., Magyar, Á., Uzinger, N., Gruiz, K., 2015. Environmental toxicity assessment of the spilled Ajka red mud in soil microcosms for its potential utilisation as soil ameliorant. *Period. Polytech. - Chem. Eng.* 59, 253.
- Ujaczki, É., Zimmermann, Y., Gasser, C., Molnár, M., Feigl, V., Lenz, M., 2017. Red mud as secondary source for critical raw materials—purification of rare earth elements by liquid/liquid extraction. *J. Chem. Technol. Biotechnol.* 92, 2835–2844.
- Ujaczki, É., Feigl, V., Molnár, M., Cusack, P., Curtin, T., Courtney, R., O'Donoghue, L., Davris, P., Hugli, C., Evangelou, M.W., Balomenos, E., 2018. Re-using bauxite residues: benefits beyond (critical raw) material recovery. *J. Chem. Technol. Biotechnol.* 93, 2498–2510.
- United States Geological Survey Website (USGS), 2016. Commodity Statistics and Information. Available: <http://minerals.usgs.gov/minerals/pubs/commodity/>. (Accessed 30 January 2018).
- Wang, S., Ang, H.M., Tade, M.O., 2008. Novel applications of red mud as coagulant, adsorbent and catalyst for environmentally benign processes. *Chemosphere* 72, 1621–1635.
- Wang, W., Pranolo, Y., Cheng, C.Y., 2013. Recovery of scandium from synthetic red mud leach solutions by solvent extraction with D2EHPA. *Sep. Purif. Technol.* 108, 96–102.
- Wang, X., Zhang, Y., Lv, F., An, Q., Lu, R., Hu, P., Jiang, S., 2015. Removal of alkali in the red mud by SO₂ and simulated flue gas under mild conditions. *Environ. Prog. Sustain. Energy* 34, 81–87.
- Weng, Z., Jowitt, S.M., Mudd, G.M., Haque, N., 2015. A detailed assessment of global rare earth element resources: opportunities and challenges. *Econ. Geol.* 110, 1925–1952.
- Xu, C., Kynický, J., Smith, M.P., Kopriva, A., Brtnický, M., Urubek, T., Yang, Y., Zhao, Z., He, C., Song, W., 2017. Origin of heavy rare earth mineralization in South China. *Nat. Commun.* 8, 14598.
- Xue, S., Kong, X., Zhu, F., Hartley, W., Li, X., Li, Y., 2016. Proposal for management and alkalinity transformation of bauxite residue in China. *Environ. Sci. Pollut. Res.* 23, 12822–12834.
- Xue, S., Li, M., Jiang, J., Millar, G.J., Li, C., Kong, X., 2018. Phosphogypsum stabilization of bauxite residue: conversion of its alkaline characteristics. *J. Environ. Sci.* <https://doi.org/10.1016/j.jes.2018.05.016>.
- Zhu, F., Liao, J., Xue, S., Hartley, W., Zou, Q., Wu, H., 2016a. Evaluation of aggregate microstructures following natural regeneration in bauxite residue as characterized by synchrotron-based X-ray micro-computed tomography. *Sci. Total Environ.* 573, 155–163.
- Zhu, F., Xue, S., Hartley, W., Huang, L., Wu, C., Li, X., 2016b. Novel predictors of soil genesis following natural weathering processes of bauxite residues. *Environ. Sci. Pollut. Res.* 23, 2856–2863.
- Zhu, F., Cheng, Q., Xue, S., Li, C., Hartley, W., Wu, C., Tian, T., 2018. Influence of natural regeneration on fractal features of residue microaggregates in bauxite residue disposal areas. *Land Degrad. Dev.* 29, 138–149.